RSC Advances

PAPER

View Article Online
View Journal | View Issue

Cite this: *RSC Adv.*, 2016, **6**, 80296

Fidelity quantification of mercury(II) ion *via* circumventing biothiols-induced sequestration in enzymatic amplification system†

Yue Zhao, Huaqing Liu, Feng Chen, Min Bai and Yongxi Zhao*

Received 1st July 2016
Accepted 11th August 2016

DOI: 10.1039/c6ra16960k

www.rsc.org/advances

Mercury(II) ion (Hg^{2+}) is a hazardous pollutant with distinct toxicological profiles that can cause deleterious effects on human health and the environment even at low concentrations, so an accurate detection method with high sensitivity is of great importance. Compared with traditional techniques requiring sophisticated instrumentation and skilled personnel, Hg^{2+} sensors based on nucleic acids amplification outperform others due to their efficiency, robustness, and ease of operation. Among these nucleic acids amplification-based strategies, a common problem meriting attention is that biothiols such as dithiothreitol (DTT) extensively exist in enzymatic amplification systems as essential components to guarantee tool enzyme activity. However, due to the high affinity of Hg^{2+} and S-donor atoms, biothiols tend to sequestrate Hg^{2+} and are probably present to affect the accuracy of detection. Herein, a fidelity quantification of Hg^{2+} based on nucleic acids amplification is developed *via* a redox reaction or DNA architecture probe. Upon circumventing a biothiols-induced sequestration in enzymatic amplification system, the proposed strategy exhibits excellent accuracy and sensitivity with a detection limit down to 300 pM.

Introduction

Hg^{2+} is a hazardous pollutant with deleterious effects on human health and the environment even at low concentrations.[1,2] So an accurate method with high sensitivity is imperative for its monitoring. Recently, thymine (T)–Hg^{2+}–T coordination is extremely fascinating in the development of Hg^{2+} sensors due to its strong interaction, which is even more stable than the Watson–Crick adenine (A)–T pair.[3,4] Serving as an emerging signal amplification tool, nucleic acids amplification rapidly accumulates sequences of interest and dramatically enhances analytical sensitivity,[5–12] Ascribed to its efficiency, robustness, and ease of operation, various nucleic acids amplification-based strategies have been proposed for Hg^{2+} detection.[13–20]

Among the methods above, a common problem meriting attention is that biothiols such as DTT and bovine serum albumin extensively exist in enzymatic amplification systems as essential components to guarantee tool enzyme activity.[21–24] But in the meantime, biothiols are also utilized to sequestrate Hg^{2+} through disassembling the T–Hg^{2+}–T bridge due to the high affinity of Hg^{2+} and S-donor atoms,[25–27] thus resulting in a serious interference to the quantification of Hg^{2+}. Thus, the development of highly sensitive and accurate biosensors of Hg^{2+} based on nucleic acids amplification is still urgently needed.

Experimental section

Reagents and materials

Mercury perchlorate trihydrate ($Hg(ClO_4)_2 \cdot 3H_2O$) was purchased from J&K Chemical Ltd. (Beijing, China). NaAc, KAc, $CaCl_2$, $NiSO_4$, $Mg(Ac)_2$, $MnSO_4$, $CuCl_2$, $Pb(NO_3)_2$, $ZnCl_2$, $CdCl_2$, $FeCl_3$, $AlCl_3$, Tris(hydroxymethyl)aminomethane (Tris), 3-(*N*-morpholino)-propanesulfonic acid (MOPS) and other chemicals were ordered from Sinopharm Chemical Reagent Co., Ltd. (Shanghai, China). Klenow Fragment (exo^-), Nt.BbvCI and their corresponding buffer were obtained from New England Biolabs Ltd. (Beijing, China). All solutions were prepared and diluted with Milli-Q water (resistance > 18.2 MΩ). All the oligonucleotides were synthesized by Sangon Biotechnology Co., Ltd. (Shanghai, China), and the sequences are as follows:

Primer 1: 5′-TAGAGGTT-3′;
Primer 2: 5′-TTGAGGTA-3′;
Complementary primer: 5′-TAGAGGTA-3′;
Three-way junction (3-WJ) probe 1:
5′-AGAGGTAGTAGGTGATAGTCGG-3′;
3-WJ probe 2: 5′-CCGTCTTTCTCCCCATAT-3′;
3-WJ template: 5′-TGAGGCTAGAGCGA**GCTGAGG**C
GGATATGGAATACTACCTCTAAA-3′;
Linear template: 5′-CAGTGAGGCTAGAGCGA**GCTGA**

The Key Laboratory of Biomedical Information Engineering of Ministry of Education, School of Life Science and Technology, Xi'an Jiaotong University, Xi'an, Shaanxi 710049, P. R. China. E-mail: yxzhao@mail.xjtu.edu.cn

† Electronic supplementary information (ESI) available: Additional figures. See DOI: 10.1039/c6ra16960k

GGCGGATATGGAATACTACCTCTAAA-3′;
Molecular beacon (MB): 5′-FAM-CCACGAGTGT**GCT GAGG**CTAGAGCGTGG-DABCYL-3′;

The bold letters represent the recognition sequence of Nt.BbvCI, and the 5′ end and 3′ end of the MB are labeled with fluorescein (FAM) and quencher (DABCYL), respectively.

Apparatus

The melting curves analyses were performed with LightCycler 96 (Roche Applied Science, Mannheim, Germany). Syngene G:BOX Imaging System (Syngene System, Cambridge, UK) was used to image gel electrophoresis. Fluorescence measurements were carried out on FluoroMax-4 fluorescence spectrometer (Horiba Jobin Yvon, Edison, NJ). Excitation and emission wavelengths were set at 494 nm and 520 nm with the slit widths of 5 nm, respectively. The emission spectra were monitored from 510 nm to 600 nm in steps of 1 nm.

Analysis of samples

The concentration of stock Hg^{2+} is 10 mM, which was dissolved in 0.5% HNO_3, and further diluted to desired concentration with 10 mM MOPS solution (pH = 7.0) containing 0.1 M $NaNO_3$.

Gel electrophoresis and melting curve analysis. The extension reaction was carried out in Tris–Ac buffer (10 mM Tris, 75 mM KAc, 10 mM $Mg(Ac)_2$, pH = 7.9) containing 100 nM primer (primer 1 or primer 2), 100 nM template (3-WJ template), 0.5 units Klenow Fragment, 0.2 × SYBR Green I and 40 μM dNTPs. After addition of Hg^{2+}, the solutions were incubated at 37 °C for 5 min. Then products of the extension reaction were analyzed by agarose gel electrophoresis and melting curve.

Fluorescence measurement. The detection was carried out in a Tris–Ac buffer (10 mM Tris, 75 mM KAc, 10 mM $Mg(Ac)_2$, pH = 7.9) containing 20 nM primer (3-WJ probe 1 & 2 or Primer 1), 20 nM 3-WJ template (or Linear template), 150 nM MB, 0.5 units Klenow Fragment, 4 units Nt.BbvCI and 40 μM dNTPs. After addition of various concentrations of Hg^{2+}, the solutions were incubated at 37 °C for 1 h. Then, fluorescence emission spectra were recorded as described above.

Results and discussion

To circumvent the biothiols-induced sequestration of Hg^{2+} in polymerase reaction, several studies make compromises through reducing the concentration of DTT in reaction buffers on the basis of commercially available reaction solutions.[16,19,28,29] Nevertheless, in stock buffers, tool enzyme is always accompanied by DTT which is unable to be changed or removed. As shown in Fig. 1A, the Hg^{2+} binding site is denoted as green in primer. Theoretically, induced by the T–Hg^{2+}–T coordination (circled by dash line), primer should offer a complementary 3′ terminal to initiate polymerization. Whereas indeed, due to the sequestration by DTT introduced from polymerase, the signal response is almost the same with blank control. In view of biothiols' reducibility and based on the reported methods, we tried to scavenge DTT by oxidation, which is a more effective approach to avoid the interferences of biothiol in both reaction buffer and tool enzymes' stock buffers at the same time. Hydrogen peroxide (H_2O_2) was preferentially taken into account for its non-interference in standard polymerase reaction (with complementary primer) at the selected concentration (Fig. S1, ESI†) and the reduction product is also compatible (mechanism of the redox reaction was shown in Fig. S2, ESI†).[30,31] As expected, Fig. 1B presents an observable signal response both in gel electrophoresis and melting curve analysis after treatment with H_2O_2, indicating the interference of DTT could be effectively eliminated. To confirm the roles of H_2O_2 and DTT in this system, we further added extra DTT into the polymerase reaction recovered by H_2O_2 and obtained an undetectable signal. Then H_2O_2 with higher concentration was brought in to consume excess DTT, resulting in a signal restoration again (Fig. 1C). As a kind of common oxidant, the H_2O_2 involved approach is universal and can be directly applied to various kinds of amplification strategies. Though this proposed strategy achieves a desired result, the involvement of readily degradable H_2O_2 is likely to lead reproducibility problems with the assay. What's more, excess H_2O_2 causes side-effects and even inhibits the signal response (Fig. S3, ESI†).

Inspired by the distinct gap between polymerase's exceptional catalytic velocity (at rates near 1000 nucleotides per minute per molecule of enzyme)[32] and biothiols' gradual competition process,[33–35] we propose another alternative strategy herein. A rational designed DNA architecture probe first

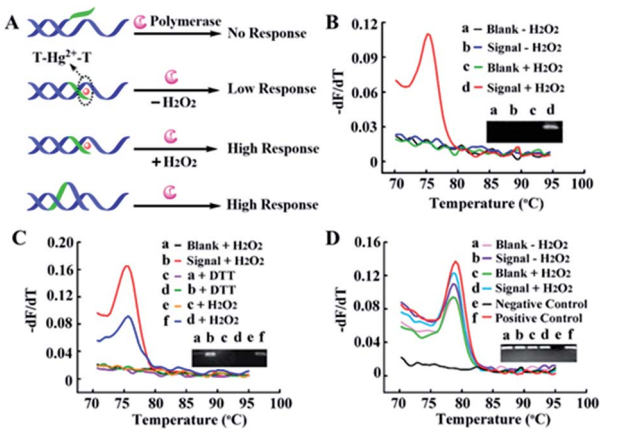

Fig. 1 (A) Illustration of the approaches to circumvent biothiols-induced sequestration of Hg^{2+} in polymerase reaction. (B) Gel electrophoresis and melting curve analysis of polymerase reaction using duplex probe with Hg^{2+} binding site at the 3′ terminal of primer in the presence of Hg^{2+} before (b) and after (d) the addition of H_2O_2 (0.01%), with corresponding blank controls without Hg^{2+} (a, c), respectively. (C) The effect of H_2O_2 and DTT on the polymerase reaction: the signal response of Hg^{2+} (b) disappears with the addition of DTT (10 μM, d) and can be recovered again after treatment with higher concentration H_2O_2 (0.02%, f), with corresponding blank controls without Hg^{2+} (a, c, e), respectively. (D) Gel electrophoresis and melting curve analysis of polymerase reaction using duplex probe with 6 bp complementary region from Hg^{2+} binding site to the 3′ terminal of primer in the presence of Hg^{2+} before (b) and after (d) the addition of H_2O_2 (0.01%), with corresponding blank controls without Hg^{2+} (a, c), respectively. Negative (e) and positive (f) control represent the polymerase reaction without and with complementary primer.

initiates extension upon Hg^{2+} binding, and immediately forms a stable polymerizable structure which is insusceptible to the subsequent Hg^{2+} release, providing another avenue to avoid the interference of biothiols. To exert a maximum advantage of catalytic rate, we reserved a perfectly complementary region with a length of 6 bp to match the minimal primer length required for polymerase,[36] so as to spatially separate the Hg^{2+} binding domain and polymerase recognition domain. A primer-template duplex probe is not a candidate due to its unwanted background, even though it shows a significant signal response in the presence of DTT (Fig. 1D).

Compared with a duplex probe, a DNA machine assembled by three strands offers an excellent discrimination of even single-base mismatched sequences,[37] and thus holds great potential to reduce the system's background amplification. Based on our previous studies about DNA architecture probes and their thermodynamics properties,[38,39] we constructed a Hg^{2+}-triggered 3-WJ DNA machine which can circumvent biothiols-induced sequestration in an enzymatic amplification system without introducing any extra interference. As illustrated in Fig. 2A, 3-WJ probes and a 3-WJ template are involved in this proposed sensing strategy. In the absence of Hg^{2+}, no stable 3-WJ DNA machine is generated to initiate the subsequent amplification. Once the Hg^{2+}-triggered 3-WJ DNA machine forms (Hg^{2+} binding site is circled by a dashed line and highlighted in pink), polymerase immediately starts extension along the 3-WJ template and produces a duplex region containing a sequence-specific nicking site (highlighted in orange) for the nicking endonuclease Nt.BbvCI to initiate a new extension cycle. Ascribed to the tactful design, numerous DNA products are continuously produced upon repeated scission and replication, even if the 3-WJ structure may have been broken up by biothiols. These products can anneal with the MB (hybridization regions are highlighted in blue) and lead to a significant fluorescence signal. On the basis of linear amplification, we introduced a recognition sequence of Nt.BbvCI within the MB, by which the next stage amplification can be coupled and generate more DNA products to open MB (hybridization regions are highlighted in magenta). Eventually, two stage amplification modules are integrated into a quadratic amplification system without adding any extra reaction components or processes. Then we compared the fluorescence responses of different amplification modes in the presence of 20 nM Hg^{2+}. In the linear process, extra 3 bases are added at the 5′ terminal of the quadratic template to block the next stage amplification. As presented in Fig. 2B, the quadratic mode exhibits a signal enhancement of 11.4 fold, whereas only a 4.6-fold signal increase is achieved by the linear mode. To confirm the feasibility of the 3-WJ DNA machine to circumvent the biothiols-induced sequestration of Hg^{2+}, a series of experiments was performed for comparing the signal responses in different systems without the treatment of H_2O_2. As shown in Fig. 2C, the 3-WJ DNA machine induces an excellent fluorescence signal enhancement, yet no detectable signal is obtained using the duplex probe with a Hg^{2+} binding site at the 3′ terminal of the primer.

To obtain the best sensing performance, the ionic strength of buffer solution (Fig. S4, ESI†), concentration of MB (Fig. S5, ESI†),

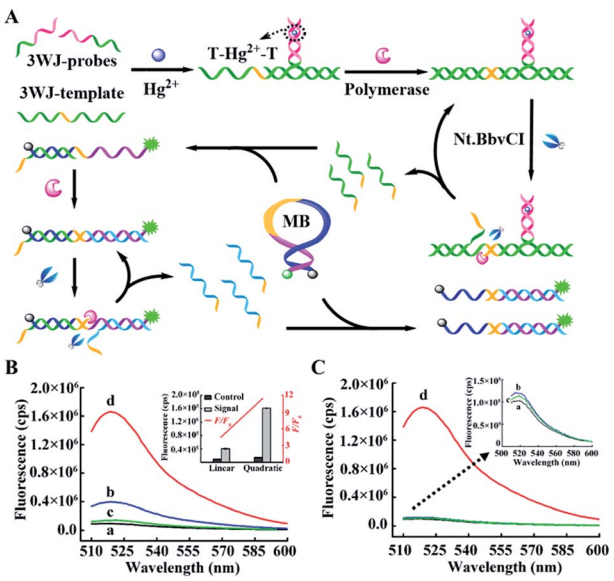

Fig. 2 (A) Illustration of Hg^{2+} detection based on 3-WJ DNA machine. (B) The fluorescence spectra of the linear (b) and quadratic (d) amplification in the presence of 20 nM Hg^{2+}, with corresponding backgrounds control without Hg^{2+} (a, c), respectively. Inset: fluorescence responses of linear and quadratic amplification. F_0 and F represent the fluorescence intensity in the absence and presence of Hg^{2+}, respectively. (C) Confirmation the feasibility of 3-WJ DNA machine to circumvent the biothiols-induced sequestration of Hg^{2+}. The fluorescence spectra of the duplex probe-mediated (with Hg^{2+} binding site at the 3′ terminal of primer, b) and 3-WJ DNA machine-mediated (d) quadratic amplification in the presence of 20 nM Hg^{2+}, with corresponding backgrounds control without Hg^{2+} (a, c), respectively. Inset is the enlargement for fluorescence spectra of (a), (b) and (c).

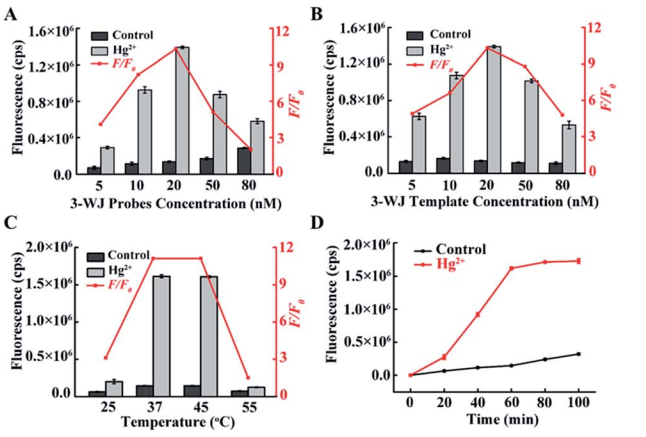

Fig. 3 Optimization of experimental conditions. The effect of the 3-WJ probes concentration (A), 3-WJ template concentration (B), and reaction temperature (C) on the fluorescence responses of proposed strategy. F_0 and F represent the fluorescence intensity in the absence and presence of 20 nM Hg^{2+}, respectively. (D) The time-dependent fluorescence response with 20 nM Hg^{2+} over background fluorescence. The error bars indicate the standard deviations of three independent experiments.

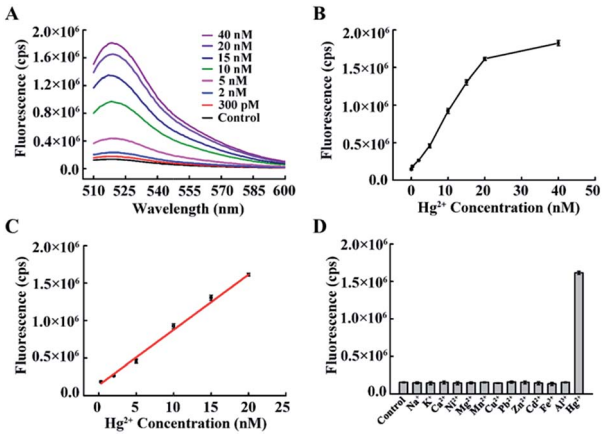

Fig. 4 (A) Fluorescence spectra response to different concentrations of Hg^{2+}. (B) Changes in fluorescence intensity at 520 nm upon the addition of various concentrations of Hg^{2+}. (C) The linear correlation between the fluorescence intensity and the concentration of Hg^{2+} in the range of 300 pM to 20 nM. (D) Selectivity of the proposed strategy for Hg^{2+} detection over other common interference metal ions. The concentration of Hg^{2+} is 20 nM, whereas the concentrations of other metal ions are each 2 μM. The error bars indicate the standard deviations of three independent experiments.

Klenow Fragment (Fig. S6, ESI†), and Nt.BbvCI (Fig. S7, ESI†) were investigated at a fixed Hg^{2+} concentration of 20 nM. As a result, 75 mM KAc, 10 mM Mg $(Ac)_2$, 150 nM MB, 0.5 units Klenow Fragment, and 4 units Nt.BbvCI were selected for the maximum fluorescence enhancement (F/F_0). Apart from the aforementioned parameters, the concentration of 3-WJ probes and 3-WJ template, reaction temperature, and time are also critical factors in this sensing strategy. With the reactant concentration increasing, more successful molecular collisions occur and speed up the rate of reaction. As shown in Fig. 3A, with the concentration of 3-WJ probes varying from 5 to 80 nM, the fluorescence intensity gradually increases and reaches a maximum at 20 nM. Thereafter, fluorescence response exhibits a decline with further increase in the concentration of the 3-WJ probes. It is possible that a certain amount of Hg^{2+} disperses among the excess probes, thus disturbing the formation of a stable 3-WJ DNA machine. As similarly presented in Fig. 3B, the fluorescence response trends to increase with the concentration of 3-WJ templates. However, high concentration templates offer more available locations to anneal amplification products which will compete with MB and reduce the signal responses, so 20 nM 3-WJ probes and 3-WJ template were chosen for the following experiments. An appropriate reaction temperature is not only closely related with the assembly of 3-WJ DNA machine, but also able to ensure the activity of enzyme. With comparison of the F/F_0 ratios at four temperatures, 37 °C was selected as the optimum temperature (Fig. 3C). In addition, the effect of the reaction time was also investigated. As depicted in Fig. 3D, the fluorescence intensity of both signal and background increases gradually with the prolongation of the reaction time. The signal intensity nearly approaches a steady state after incubation for 60 min, while background intensity continues to rise. Thus, 60 min was selected as the optimized reaction time.

Under the optimized detection conditions, various concentrations of Hg^{2+} (0–40 nM) were introduced into the system to examine whether the proposed strategy could be used for quantification. With increase of the Hg^{2+} concentration, the fluorescence spectrum appears as an obvious enhancement accordingly (Fig. 4A). The relationship between the fluorescence intensities at 520 nm and the concentrations of Hg^{2+} is shown in Fig. 4B. As depicted in Fig. 4C, a good linear relationship between the fluorescence intensity and the Hg^{2+} concentration is obtained in the range from 300 pM to 20 nM, with a regression equation of $Y = 0.7368X + 1.4087$ and a correlation coefficient of 0.9933, where Y is the fluorescence intensity ($\times 10^5$ cps) and X is the Hg^{2+} concentration, indicating that the fluorescence sensing strategy is effective for the detection of Hg^{2+}. The limit of detection (taken to be 3 times the standard deviation in the blank solution) is 300 pM, which is lower than the maximum level of Hg^{2+} in drinking water permitted by the U.S. Environmental Protection Agency (10 nM). To the best of our knowledge, this detection limit of the proposed approach is much lower than those of most existing colorimetric (50–60 nM)[40,41] and fluorescent (0.8–2.5 nM)[42,43] methods, and is even comparable to some electrochemical (0.2 nM)[44] and electrochemiluminescent (2.3 nM)[45] sensors.

The selectivity of the proposed sensing system for Hg^{2+} was evaluated by investigating the responses of the assay to other environmentally relevant metal ions, including Na^+, K^+, Ca^{2+}, Ni^{2+}, Mg^{2+}, Mn^{2+}, Cu^{2+}, Pb^{2+}, Zn^{2+}, Cd^{2+}, Fe^{3+}, and Al^{3+}. As shown in Fig. 4D, Hg^{2+} exhibits a remarkable fluorescence signal response and other interfering metal ions have only negligible effects even at a 100-fold concentration more than Hg^{2+} (2 μM *vs.* 20 nM), demonstrating an excellent selectivity of the proposed method over other metal ions.

To validate the capability of the proposed strategy for practical applications, we applied this assay to detect Hg^{2+} ions in water samples from the Xi'an Chan River and Xi'an Ba River.

Table 1 Results for the determination of Hg^{2+} in river water samples

Sample	Hg^{2+} added (nM)	Measured (nM)	Recovery[a] (%)	AFS (nM)	Recovery[b] (%)
Xi'an	5	5.23 ± 0.38^d	104.6	$5.48^c \pm 0.45^d$	109.0
Chan river	10	$10.35^c \pm 0.15^d$	103.5	$9.93^c \pm 0.51^d$	99.3
Xi'an	5	$4.78^c \pm 0.28^d$	95.6	$5.38^c \pm 0.34^d$	107.6
Ba river	10	$10.15^c \pm 0.43^d$	101.5	$10.33^c \pm 0.31^d$	103.3

[a] The recovery obtained by this proposed method. [b] The recovery obtained by AFS. [c] Mean of three determinations. [d] Standard deviation.

The collected water was filtered by using a 0.22 μm membrane to remove insoluble substances, and obtained an undetectable signal response of Hg^{2+}, which was confirmed by Atomic Fluorescence Spectrometry (AFS). Then the water samples were spiked with Hg^{2+} at different concentrations of 5 nM and 10 nM. As listed in Table 1, satisfactory values between 95.6% and 104.6% were obtained for the recovery experiments. Moreover, the artificially contaminated water samples were further certified by AFS, the results of which are in accordance with the proposed method, confirming the accuracy and fidelity of the developed strategy for the quantification of Hg^{2+} and indicating its great potential for real environmental samples analysis.

Conclusions

In this work, the sequestration of Hg^{2+} induced by biothiols in an enzymatic system was discussed. By using a redox reaction or DNA architecture probe, we successfully developed a strategy to circumvent interferences and obtained a fidelity quantification of Hg^{2+}. Through a well-designed MB, we introduced a homogeneous and quadratic amplification strategy and achieved an excellent sensitivity with a detection limit of 300 pM. In addition, the proposed sensing system displayed an extreme specificity towards Hg^{2+}, even in the presence of 100-fold excess of other interfering metal ions due to the specific formation of T–Hg^{2+}–T coordination. Furthermore, the method's accuracy and reliability for the detection of Hg^{2+} in complex water samples was verified by AFS, demonstrating the sensing strategy has enormous potential in real environmental samples.

Acknowledgements

This research was supported by the Research Project Foundation of Shaanxi Branch of China National Tobacco Corporation (No. 201112029), the National Natural Science Foundation of China (No. 21475102) and "Young Talent Support Plan" of Xi'an Jiaotong University. We would like to thank Engineer Guanghui Qiang at Xi'an Water Group Company Limited (Xi'an, Shaanxi) for supporting the AFS analysis.

Notes and references

1 P. M. Bolger and B. Schwetz, *N. Engl. J. Med.*, 2002, **347**, 1735–1736.
2 T. W. Clarkson, L. Magos and G. J. Myers, *N. Engl. J. Med.*, 2003, **349**, 1731–1737.
3 A. Ono and H. Togashi, *Angew. Chem., Int. Ed.*, 2004, **43**, 4300–4302.
4 Y. Miyake, H. Togashi, M. Tashiro, H. Yamaguchi, S. Oda, M. Kudo, Y. Tanaka, Y. Kondo, R. Sawa and T. Fujimoto, *J. Am. Chem. Soc.*, 2006, **128**, 2172–2173.
5 Y. Zhao, F. Chen, Q. Li, L. Wang and C. Fan, *Chem. Rev.*, 2015, **115**, 12491–12545.
6 Y. Zhao, F. Chen, Q. Zhang, Y. Zhao, X. Zuo and C. Fan, *NPG Asia Mater.*, 2014, **6**, e131.
7 R. Deng, L. Tang, Q. Tian, Y. Wang, L. Lin and J. Li, *Angew. Chem., Int. Ed.*, 2014, **53**, 2389–2393.
8 Z. Ge, M. Lin, P. Wang, H. Pei, J. Yan, J. Shi, Q. Huang, D. He, C. Fan and X. Zuo, *Anal. Chem.*, 2014, **86**, 2124–2130.
9 W. Li, Z. Liu, H. Lin, Z. Nie, J. Chen, X. Xu and S. Yao, *Anal. Chem.*, 2010, **82**, 1935–1941.
10 X. Zhang, C. Liu, L. Sun, X. Duan and Z. Li, *Chem. Sci.*, 2015, **6**, 6213–6218.
11 Y. Zhang, L. Zhang, J. Sun, Y. Liu, X. Ma, S. Cui, L. Ma, J. J. Xi and X. Jiang, *Anal. Chem.*, 2014, **86**, 7057–7062.
12 R. Duan, X. Zuo, S. Wang, X. Quan, D. Chen, Z. Chen, L. Jiang, C. Fan and F. Xia, *J. Am. Chem. Soc.*, 2013, **135**, 4604–4607.
13 J. Liu, L. Chen, J. Chen, C. Ge, Z. Fang, L. Wang, X. Xing and L. Zeng, *Anal. Methods*, 2014, **6**, 2024–2027.
14 X. Zhou, Q. Su and D. Xing, *Anal. Chim. Acta*, 2012, **713**, 45–49.
15 L. Freage, F. Wang, R. Orbach and I. Willner, *Anal. Chem.*, 2014, **86**, 11326–11333.
16 D. Li, A. Wieckowska and I. Willner, *Angew. Chem.*, 2008, **120**, 3991–3995.
17 H. Jia, Z. Wang, C. Wang, L. Chang and Z. Li, *RSC Adv.*, 2014, **4**, 9439–9444.
18 G. Zhu, Y. Li and C.-Y. Zhang, *Chem. Commun.*, 2014, **50**, 572–574.
19 X. Zhu, X. Zhou and D. Xing, *Biosens. Bioelectron.*, 2011, **26**, 2666–2669.
20 J. Yin, X. He, X. Jia, K. Wang and F. Xu, *Analyst*, 2013, **138**, 2350–2356.
21 W. Cleland, *Biochemistry*, 1964, **3**, 480–482.
22 S. Shah, A. Sharma and M. N. Gupta, *Anal. Biochem.*, 2006, **351**, 207–213.
23 M. Nagai, A. Yoshida and N. Sato, *IUBMB Life*, 1998, **44**, 157–163.
24 A. Haas and I. Rose, *J. Biol. Chem.*, 1982, **257**, 10329–10337.
25 J. M. Thomas, H.-Z. Yu and D. Sen, *J. Am. Chem. Soc.*, 2012, **134**, 13738–13748.
26 L. Wang, T. Yao, S. Shi, Y. Cao and W. Sun, *Sci. Rep.*, 2014, **4**, 5320.
27 M. Stobiecka, A. A. Molinero, A. Chałupa and M. Hepel, *Anal. Chem.*, 2012, **84**, 4970–4978.
28 H. Urata, E. Yamaguchi, T. Funai, Y. Matsumura and S. I. Wada, *Angew. Chem.*, 2010, **122**, 6666–6669.
29 T. Funai, J. Nakamura, Y. Miyazaki, R. Kiriu, O. Nakagawa, S. I. Wada, A. Ono and H. Urata, *Angew. Chem., Int. Ed.*, 2014, **53**, 6624–6627.
30 W. M. Kaiser, *Planta*, 1979, **145**, 377–382.
31 C. C. Winterbourn and D. Metodiewa, *Free Radical Biol. Med.*, 1999, **27**, 322–328.
32 A. Kornberg, *Science*, 1969, **163**, 1410–1418.
33 M. Zhang, H.-N. Le, X.-Q. Jiang and B.-C. Ye, *Chem. Commun.*, 2013, **49**, 2133–2135.
34 J. Zhao, C. Chen, L. Zhang, J. Jiang, G. Shen and R. Yu, *Analyst*, 2013, **138**, 1713–1718.
35 H. Xu and M. Hepel, *Anal. Chem.*, 2011, **83**, 813–819.
36 G. Zhao and Y. Guan, *Acta Biochim. Biophys. Sin.*, 2010, **42**, 722–728.
37 Q. Zhang, F. Chen, F. Xu, Y. Zhao and C. Fan, *Anal. Chem.*, 2014, **86**, 8098–8105.

38 Y. Zhao, L. Qi, F. Chen, Y. Zhao and C. Fan, *Biosens. Bioelectron.*, 2013, **41**, 764–770.
39 F. Chen, C. Fan and Y. Zhao, *Anal. Chem.*, 2015, **87**, 8758–8764.
40 G.-H. Chen, W.-Y. Chen, Y.-C. Yen, C.-W. Wang, H.-T. Chang and C.-F. Chen, *Anal. Chem.*, 2014, **86**, 6843–6849.
41 J. Wu, L. Li, D. Zhu, P. He, Y. Fang and G. Cheng, *Anal. Chim. Acta*, 2011, **694**, 115–119.
42 H. Xu, X. Zhu, H. Ye, L. Yu, X. Liu and G. Chen, *Chem. Commun.*, 2011, **47**, 12158–12160.
43 J. Ma, Y. Chen, Z. Hou, W. Jiang and L. Wang, *Biosens. Bioelectron.*, 2013, **43**, 84–87.
44 F. Xuan, X. Luo and I. M. Hsing, *Anal. Chem.*, 2013, **85**, 4586–4593.
45 X. Zhu, L. Chen, Z. Lin, B. Qiu and G. Chen, *Chem. Commun.*, 2010, **46**, 3149–3151.